EUKARYOTIC CELL, Apr. 2004, p. 447–458 Vol. 3, No. 2
1535-9778/04/$08.00+0 DOI: 10.1128/EC.3.2.447–458.2004

A Novel Allele of *Saccharomyces cerevisiae NDC1* Reveals a Potential Role for the Spindle Pole Body Component Ndc1p in Nuclear Pore Assembly

Corine K. Lau, Thomas H. Giddings, Jr., and Mark Winey*

MCD Biology, University of Colorado—Boulder, Boulder, Colorado

Received 16 October 2003/Accepted 22 December 2003

Both the spindle pole body (SPB) and the nuclear pore complex (NPC) are essential organelles embedded in the nuclear envelope throughout the life cycle of the budding yeast *Saccharomyces cerevisiae*. However, the mechanism by which these two multisubunit structures are inserted into the nuclear envelope during their biogenesis is not well understood. We have previously shown that Ndc1p is the only known integral membrane protein that localizes to both the SPBs and the NPCs and is required for SPB duplication. For this study, we generated a novel temperature-sensitive (*ts*) allele of *NDC1* to investigate the role of Ndc1p at the NPCs. Yeast cells carrying this allele (*ndc1-39*) failed to insert the SPB into the nuclear envelope at the restrictive temperature. Importantly, the double mutation of *ndc1-39* and NPC assembly mutant *nic96-1* resulted in cells with enhanced growth defects. While nuclear protein import and NPC distribution in the nuclear envelope were unaffected, *ndc1-39* mutants failed to properly incorporate the nucleoporin Nup49p into NPCs. These results provide evidence that Ndc1p is required for NPC assembly in addition to its role in SPB duplication. We postulate that Ndc1p is crucial for the biogenesis of both the SPBs and the NPCs at the step of insertion into the nuclear envelope.

The spindle pole body (SPB) in the budding yeast *Saccharomyces cerevisiae* is the sole microtubule organizing center of the cell. This essential multilayered organelle (26) is comprised of at least 18 different proteins (1, 9, 18, 19) and is embedded in the nuclear envelope throughout the cell cycle. The single SPB duplicates during the G_1 phase of the cell cycle, and the two resulting SPBs serve as the poles of the spindle that properly aligns and segregates the chromosomes during mitosis. The fidelity of SPB duplication is crucial to the survival of the cell since perturbations to this process can lead to genetic instability (12).

Ultrastructural studies using electron microscopy have revealed several intermediate steps during SPB duplication (1, 12). The first step is the formation of the satellite, the SPB precursor, on a modified nuclear envelope structure adjacent to the existing SPB called the half-bridge. The satellite enlarges into the duplication plaque, a partial cytoplasmic SPB structure that is then inserted into the nuclear envelope. After insertion, the nuclear SPB components are incorporated into the nascent SPB, after which duplicated side-by-side SPBs separate and migrate to the opposite ends of the nucleus.

Although it is not known how the duplication plaque is inserted into the nuclear envelope, SPB components encoded by *NDC1*, *MPS2*, and *BBP1* have been implicated at this step (32, 39, 40), and mutations in these genes cause similar SPB duplication defects. For example, cells carrying the cold-sensitive *ndc1-1* mutation are unable to insert the duplication plaque into the nuclear envelope at the restrictive temperature of 15°C (40). The cells arrest transiently in mitosis with a monopolar spindle but eventually go through mitosis without proper DNA segregation and produce polyploid, aploid, or aneuploid daughter cells (35, 40).

NDC1 encodes an essential integral membrane protein with 6 or 7 predicted transmembrane domains (11, 40). As previously reported, yeast cells are very sensitive to *NDC1* gene dosage (10). For example, overexpression of *NDC1* causes cells to exhibit SPB duplication defects similar to that observed for *ndc1-1* mutants. In addition, *NDC1* is one of the few genes in yeast that is haplo-insufficient, meaning diploid cells are not viable with only one chromosomal copy of *NDC1*. Ndc1p and its orthologue, Cut11p of *Schizosaccharomyces pombe*, are unique in that they are the only known integral membrane proteins that localize to both the SPBs and the nuclear pore complexes (NPCs) (11, 38). While roles for Ndc1p and Cut11p at SPBs have been established through the use of conditional alleles, no NPC-associated functions such as nuclear protein import, mRNA export, NPC distribution, or NPC assembly have been observed thus far (11).

The NPC controls the trafficking of macromolecules between the cytoplasm and the nucleus. Approximately 30 different proteins make up the NPC, which contains a ring of eight symmetrical spokes surrounding a central transporter (28, 34, 36, 43). In addition, structures such as the cytoplasmic filaments and nuclear filaments, which connect to form a nuclear pore basket, are important for facilitating cargo docking and transport. In yeast, both the NPCs and the SPBs are inserted into the nuclear envelope during their biogenesis, but unlike SPB duplication, NPCs are synthesized continuously throughout the cell cycle (41). Although subcomplexes of nuclear pore proteins, or nucleoporins, have been identified (34), the assembly mechanism of the nucleoporins into NPCs is not well understood. Nonetheless, studies from vertebrate models suggest that integral membrane proteins are crucial during

* Corresponding author. Mailing address: MCD Biology, University of Colorado—Boulder, Boulder, CO 80309-0347. Phone: (303) 492-3409. Fax: (303) 492-7744. E-mail: Mark.Winey@colorado.edu.

TABLE 1. Yeast strains

Strain	Relevant genotype	Reference or source
1258	MAT**a** *nup133*Δ::*HIS3 nup49-1*::*URA3-nup49*Δ*GLFG*::*GFP-S65T-TRP1 ade2-1*::*ADE2-URA3* (SWY828)	7
1264	MATα *NDC1*	5
2252	MAT**a** nic96::HIS3 + pUN100-LEU2-nic96-1	44
2568	MAT**a** *NDC1*	This study
2709	MATα *ndc1*Δ::*KanMX* + pALR10-NDC1	This study
2710	MAT**a** *ndc1*Δ::*KanMX*::*ndc1-39-TRP1*	This study
2804	MAT**a** *SPC42-GFP-KanMX4 LYS2*	This study
2925	MATα *prp20-1 leu2 trp 1 ura3* (PSY713)	This study
3244	MAT**a**/α *ndc1*Δ::*KanMX*::*ndc1-39-TRP1*/*ndc1*Δ::*KanMX*::*ndc1-39-TRP1 GAL10-GFP-S65T-nup49-URA3*/*GAL10-GFP-S65T-nup49-URA3* + pSW240 (pRS423-NUP49)	21
3245	MAT**a**/α *GAL10-GFP-S65T-nup49-URA3*/*GAL10-GFP-S65T-nup49-URA3* + pSW240	This study; 6
3299	MAT**a**/α *ndc1-1*/*ndc1-1 GAL10-GFP-S65T-nup49-URA3*/*GAL10-GFP-S65T-nup49-URA3 lys2-801*/+ *trp1-1*/+ +pSW240	This study; 6
3345	MAT**a**/α *nup49-1*::*URA3-nup49*Δ*GLFG*::*GFP-S65T-TRP1*/*nup49-1*::*URA3-nup49*Δ*GLFG*::*GFP-S65T-TRP1*	This study; 6
3346	MAT**a**/α *ndcI*Δ::*KanMX*::*ndc1-39-TRP1*/*ndc1*Δ::*KanMX*::*ndc1-39-TRP1 nup49-1*::*URA3-nup49*Δ*GLFG*::*GFP-S65T-TRP1*/*nup49-1*::*URA3-nup49*Δ*GLFG*::*GFP-S65T-TRP1*	This study; 6
3446	MATα*ndc1*Δ::*KanMX*::*ndc1-39-TRP1*	This study
3447	MAT**a** *ndc1*Δ::*KanMX*::*ndc1-39-TRP1 SPC42-GFP-KanMX4*	This study
3448	MAT**a**/**a** *ndc1*Δ::*KanMX*::*ndc1-39-TRP1*/*ndc1*Δ::*KanMX*::*ndc1-39-TRP1 SPC42-GFP-KanMX4*/*SPC42-GFP-KanMX4*	This study
3451	MAT**a** *ndc1*Δ::*KanMX SPC42-GFP-KanMX4* +pRS314-NDC1-3xmyc	This study
3452	MAT**a** *ndc1*Δ::*KanMX SPC42-GFP-KanMX4* +pRS314-ndc1-39-3xmyc	This study
3538	MATα *ndc1*Δ::*KanMX*::*ndc1-39-TRP1* nic96::HIS3 + pUN100-LEU2-nic96-1	This study
3539	MATα *ndc1*Δ::*KanMX*::*ndc1-39-TRP1* nic96::HIS3 + pUN100-LEU2-nic96-1	This study

NPC assembly (8, 36). Interestingly, the *nic96-1* or *nup192-15* mutation or the depletion of *NSP1* in yeast causes a decrease in NPC numbers, indicating that NPC assembly is affected in these strains (15, 22, 25, 44). In addition, genetic screens have revealed that several genes involved in the Ran GTPase cycle and in endoplasmic reticulum-Golgi trafficking also affect NPC assembly (7, 29, 30). Despite the localization of Ndc1p to NPCs and the genetic interaction between *NDC1* and another pore membrane protein, encoded by *POM152*, NPC-associated functions appear to be normal in *ndc1-1* mutants (11).

For this study, we generated a novel temperature-sensitive (*ts*) allele of *NDC1*, *ndc1-39*, to address whether Ndc1p has a functional role at the NPCs. We demonstrate that *ndc1-39* causes both SPB duplication and potential NPC assembly defects and provide evidence that Ndc1p, the only pore membrane protein essential for viability in the budding yeast, may be required for NPC assembly.

MATERIALS AND METHODS

Yeast strains and media. The yeast strains used for this study are listed in Table 1. Yeast manipulations were performed by using standard techniques (16). Yeast cells were grown in YPD medium (1% yeast extract, 2% Bacto Peptone, and 2% glucose), raffinose-containing medium (1% yeast extract, 2% Bacto Peptone, and 3% raffinose), or synthetic medium with 3% raffinose or 2% glucose supplemented with appropriate amino acids. For galactose induction experiments, galactose was added to a final concentration of 3%. Plates containing 5-fluoroorotic acid (5-FOA) were made as previously described (4). Yeast cells were arrested in G_1 phase by use of synthetic α-factor peptide (Macromolecular Resources, Fort Collins, Colo.) at 11 μg/ml.

All strains generated for this study were derivatives of an S288C-based strain (*ade2*Δ::*hisG his3*Δ*200 leu2*Δ*0 lys2*Δ*0 met15*Δ*0 trp1*Δ*63 ura3*Δ*0*) (5), except strain 3299, which was a derivative of another S288C-based strain (*ade2*Δ*426 ade3*Δ *his3*Δ*200 leu2*Δ*1 lys2-801 ura3-52*). Strains 3244, 3245, and 3299 were descendants of SWY865, and strains 3345 and 3346 were descendants of SWY809 (6). Both SWY809 and SWY865 were derived from W303 (*ade2-1 can1-100 his3-11,15 leu2-3,112 trp1-1 ura3-1*).

Strain 2709 (*ndc1*Δ::*KanMX*/pALR10-NDC1) was made by use of a two-step gene replacement technique (27) to replace the *NDC1* open reading frame (ORF) of the wild-type strain (strain 1264) with *KanMX* (37). Strain 2709 also contains the pALR10-NDC1 plasmid (11). Strain 2804 (*SPC42 GFP KanMX4*) was made by tagging the endogenous *SPC42* gene at the carboxyl terminus with green fluorescent protein (GFP) by standard techniques (20).

For the isolation of *NDC1* temperature-sensitive (*ts*) alleles, an *NDC1* mutagenized library (see below) was transformed into strain 2709 (*ndc1*Δ::*KanMX*/pALR10-NDC1). Of the approximately 5,200 colonies screened, 622 were able to grow on 5-FOA-containing plates, indicating that the mutagenized copy of *NDC1* could supply *NDC1* function at the permissive temperature of 23°C. These colonies were then tested for temperature sensitivity at the restrictive temperature of 35°C. One of the three temperature-sensitive (*ts*) alleles of *NDC1* obtained (*ndc1-39*) displayed interesting phenotypes and was further characterized, and the molecular lesions of the *ndc1-39* mutant were determined.

The *ndc1-39* allele was tagged with three copies of the *myc* epitope (pRS314-ndc1-39-3xmyc) by replacing the XhoI-MscI *NDC1* fragment (contains the entire *NDC1* ORF except the last 19 amino acids) of pRS314-NDC1-3xmyc with the XhoI-MscI *ndc1-39* fragment from pRS314-ndc1-39 (originated from the mutagenized library). pRS314-ndc1-39-3xmyc was transformed into strain 2709 (*ndc1*Δ::*KanMX*/pALR10-NDC1), and then pALR10-NDC1 was removed by counterselection on a 5-FOA plate to create strain 3450.

The *ndc1-39* allele was integrated into the chromosome by use of the following method. First, pRS304-KanMX was created by subcloning the BglII-EcoRI fragment containing the *KanMX* gene from pRS400 (5) into filled NotI sites of pRS304 (33). Second, the XhoI-SpeI *ndc1-39* fragment (includes the entire *NDC1* ORF) from pRS314-ndc1-39 was cloned into pRS304-KanMX to generate pRS304-KanMX-ndc1-39. Third, pRS304-KanMX-ndc1-39 was then linearized at the EcoNI site and integrated into the *KanMX* gene of strain 2709 (*ndc1*Δ::*KanMX*/pALR10-NDC1). pALR10-NDC1 was then removed by counterselection on a 5-FOA plate to create strain 2710.

Plasmids. Circular and linearized plasmids were transformed into yeast by use of an EZ transformation kit (Zymo Research, Orange, Calif.).

All of the *NDC1* truncation constructs were made as described previously (23) and according to the pGEM Single Strand Systems manual (Promega, Madison, Wis.). First, pBS-NDC1-3xmyc was created by cloning the XhoI-SpeI fragment of *NDC1-3xmyc* (10) (GenBank number X52328) into pBluescript II SK(+) (Stratagene, La Jolla, Calif.). Next, each of the seven pairs of *NDC1* truncation oligonucleotides was used for single-strand mutagenesis to introduce two NcoI sites (underlined) into pBS-NDC1-3xmyc at various *NDC1* locations. The se-

quences of the *NDC1* truncation oligonucleotides were as follows: NDC1mut1, CAG GGC AAG CCC ATG GTA CAG ACG CC; NDC1mut85, CAA GAA AAA ATT CCA TGG ATG TAA AG; NDC1mut174, CGA AAA CTT TTC CAT GGC CCC ACA AG; NDC1mut255, CAC ATA TGT CCA TGG GTT GTC TGC AC; NDC1mut368, AAT CTA GAT TCC ATG GAT GAG AAC GG; NDC1mut466, AAA ATT CTA CCA TGG CGT TTA TTT TC; NDC1mut573, GAT CCG GAA TCC ATG GCA TAC ACT GC; and NDC1mut655, CCC TAA TGC TAC CAT GGG AGG TGA AC. The *NDC1-3xmyc*-containing XhoI-SpeI fragments from various pBS-NDC1-3xmyc plasmids with NcoI sites were cloned into pRS314 (33), followed by NcoI restriction digestion and religation, to generate the following seven *NDC1* truncations:pRS314-ndc1Δ1-85-3xmyc, pRS314-ndc1Δ85-174-3xmyc, pRS314-ndc1Δ174-255-3xmyc, pRS314-ndc1Δ255-368-3xmyc, pRS314-ndc1Δ368-466-3xmyc, pRS314-ndc1Δ466-573-3xmyc, and pRS314-ndc1Δ573-655-3xmyc. The junctions of all *NDC1* truncations were verified by sequence analysis.

For generation of an *NDC1* mutagenized library, the *NDC1* ORF was PCR amplified with primers 5′*Xho*I-NDC1 (CCG ATT CTC GAG TAC CGG TCG CGT AAC CCG [the XhoI site that was created is underlined]) and NDC1-P (CAT TCT TGC CAA TTC GGC TC). The following were added to each of the nine 20-μl independent PCR mixtures: 30 ng of pRS315-NDC1 (10), a 0.5 mM concentration of each deoxynucleoside triphosphate, 3 mM $MgCl_2$, a 1 μM concentration of each primer, 0.5 mM $MnCl_2$, and 2.5 U of *Taq* DNA polymerase (Invitrogen, Carlsbad, Calif.). After incubation at 95°C for 5 min, the reactions were subjected to 35 cycles of 95°C for 1 min, 53°C for 1 min, and 72°C for 3 min, followed by incubation at 72°C for an additional 7 min. The PCR products were pooled, gel purified by use of a Qiagen gel extraction kit (Qiagen, Valencia, Calif.), digested with XhoI and SpeI, and cloned into pRS314. Approximately 2,300 individual bacterial colonies were pooled, and plasmid DNAs were isolated to generate the *NDC1* mutagenized library.

Flow cytometry. Flow cytometry was performed as described previously (17), with propidium iodide used to stain DNA. Cells were analyzed in a FACScan flow cytometer, and the Cell Quest software package was used for data analysis (Becton-Dickinson, San Jose, Calif.).

Cytological techniques. Immunofluorescence (IF) microscopy was performed as described previously (11). Cells containing Myc-epitope-tagged wild-type Ndc1p, truncated Ndc1p, and Ndc1-39p were fixed in 3.7% formaldehyde for 5 min, followed by rinsing with PBSA (10 mg of NaCl/ml, 0.2 mg of KCl/ml, 1.43 mg of KH_2PO_4/ml). The cells were then incubated in spheroplasting solution (4.83 μg of Zymolyase 100T/ml, 0.1 M β-mercaptoethanol in 1.2 M sorbitol, 100 mM KPO_4 [pH 7.5]) for 30 min at 30°C. After being rinsed with PBSA, the spheroplasted cells were spotted onto poly-L-lysine-treated microscope slides. The slides were submerged into 100% methanol on ice for a few seconds before being allowed to equilibrate to room temperature. The slides were then submerged into acetone for 30 s at room temperature and dried. Blocking solution (PBSA with 10 mg of bovine serum albumin/ml and 0.1% Tween 20) was applied to the slides before they were treated with a rabbit anti-Myc primary antibody (1:1,000; a gift from Don Cleveland, Ludwig Institute for Cancer Research, La Jolla, Calif.) overnight at 4°C. After the slides were rinsed with PBSA, a Cy3-conjugated donkey anti-rabbit secondary antibody (1:2,000; Jackson ImmunoResearch Laboratories, Inc., West Grove, Pa.) was applied for 2 h at room temperature in the dark. DNAs were stained with 4′,6-diamidino-2-phenylindole (DAPI) (Sigma Chemical Company, St. Louis, Mo.) and the slides were mounted in Citifluor (Ted Pella Inc., Redding, Calif.).

Cells containing Spc42p-GFP were processed as described above, except that they were fixed in 3.7% formaldehyde for 45 min and the microscope slides were not treated with methanol and acetone. Microtubules were labeled with YOL1/34 rat anti-α-tubulin primary antibody (1:150; Accurate Chemical and Scientific Corporation, Westbury, N.Y.), and a Texas red-conjugated donkey anti-rat secondary antibody (1:300; Jackson ImmunoResearch Laboratories, Inc.). Spc42p-GFP was visualized by GFP autofluorescence, and DNAs were visualized by staining with DAPI. Cells containing GAL-H2B1-GFP or constitutively expressed Nup49p-GFP were fixed in 3.7% formaldehyde for 5 min, followed by 20 min in DAPI, to visualize GFP autofluorescence and DNA. Cells containing GAL-Nup49p-GFP were visualized directly without fixation.

Standard fluorescence microscopy was carried out with a Leica DMRXA/RF4/V automated microscope equipped with a SensiCam CCD digital camera (Cooke, Tonawanda, N.Y.), and digital images were processed with Slidebook software (version 3.0.3.1; Intelligent Imaging Innovations, Denver, Colo.).

Immunoelectron microscopy (IEM) experiments were performed as described previously (14). Samples were frozen under high pressure in a BAL-TEC HPM-010 high-pressure freezer, freeze-substituted in 0.25% glutaraldehyde and 0.05% uranyl acetate in acetone, and embedded in Lowicryl HM20, and 60-nm-thick sections were collected on Formvar-coated nickel slot grids. The grids were then floated on blocking solution (1% nonfat dry milk in phosphate-buffered saline with Tween 20) and labeled with an affinity-purified rabbit anti-GFP primary antibody (diluted 1:100 in blocking solution) (a gift from Jason Kahana, Ludwig Institute for Cancer Research, and Pamela Silver, Dana-Farber Cancer Institute, Boston, Mass.) (45). Next, a goat anti-rabbit secondary antibody conjugated to 15-nm-diameter colloidal gold beads (diluted 1:20 in blocking solution; Ted Pella Inc.) was applied. The grids were stained with uranyl acetate and lead citrate and were visualized in a Philips CM10 or Philips Technai F20 electron microscope operating at 80 kV.

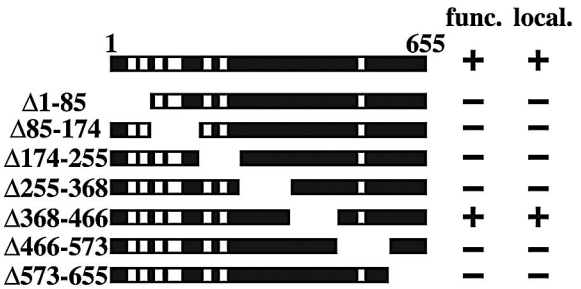

FIG. 1. The majority of the *NDC1* gene is required for its function. *NDC1* encodes a protein of 655 amino acids, and the structure of *NDC1* includes seven predicted transmembrane domains, represented as white bars. The various *NDC1* truncations are shown below the full-length *NDC1*. The ability of the *NDC1* truncations to complement an *NDC1* null strain (func.) was tested by the competence of *ndc1*Δ::*KanMX*/pALR10-NDC1 cells (strain 2709) to grow on 5-FOA plates in the presence of each of the seven *NDC1* truncation plasmids. −, cells containing the *NDC1* truncation construct cannot grow in the absence of the wild-type *NDC1* plasmid; +, cells containing the *NDC1* truncation construct can grow in the absence of the wild-type *NDC1* plasmid. The subcellular localization (local.) of the various *NDC1* truncations was determined by IF microscopy (see Materials and Methods). −, *NDC1* truncations are not localized to the SPBs or NPCs; +, the *NDC1* truncation is localized correctly to the SPBs and NPCs.

RESULTS

The majority of the *NDC1* gene is required for its function. Ndc1p was previously shown to localize to both the SPBs and NPCs (11). In order to further elucidate the role of *NDC1* in both SPB duplication and NPC-associated functions, we constructed seven serial deletion mutations in *NDC1* (Fig. 1; also see Materials and Methods), with each containing three copies of the Myc epitope tag at the carboxy terminus. The seven serial *NDC1* truncations were assayed for the ability to complement an *ndc1*Δ strain (Fig. 1). Only the *NDC1* truncation Δ368-466 provided sufficient *NDC1* functioning for viability, while *NDC1* truncations Δ1-85, Δ85-174, Δ174-255, Δ255-368, Δ466-573, and Δ573-655 did not. All of the *NDC1* truncation proteins were expressed at the same level as the wild-type protein, as assessed by Western blot analysis (data not shown), except for the *NDC1* truncations Δ1-85 and Δ255-368, whose expression was reduced severalfold and therefore whose contribution to functioning cannot be evaluated unambiguously. Consistent with the assay for functioning, only *NDC1* truncation protein Δ368-466 localized correctly to the SPBs and the NPCs (Fig. 1 and data not shown), whereas the other six *NDC1* truncation proteins were visible neither at the SPBs nor the NPCs. In summary, most of Ndc1p, except the region between amino acids 368 and 466, appears to be essential for its proper localization and functioning. Furthermore, cells containing the

Δ368-466 truncation allele did not exhibit any conditional phenotypes, so they were not analyzed further.

***ndc1-39* is a novel *ts* allele of *NDC1*.** An *NDC1* mutagenized library was generated by error-prone PCR as an alternative approach to create *ts* alleles of *NDC1* (see Materials and Methods) because the truncation alleles did not yield a conditional allele and did not point to a specific region of *NDC1* for mutagenesis. We isolated the *ndc1-39 ts* allele by screening *NDC1* mutagenized clones that caused cells to display temperature sensitivity at 35°C. When the *ndc1-39* allele was sequenced, six mutations (T14M, F218V, L288M, E293G, M457T, and F643L) were identified within the ORF (Fig. 2A). While triple (F218V, L288M, and E293G) or quadruple (T14M, F218V, L288M, and E293G) mutations were able to produce the *ts* phenotype, pair-wise mutations (T14M and F218V, L288M and E293G, or M457T and F643L) were not (data not shown). Therefore, F218V, L288M, and E293G together were sufficient to cause the *ts* phenotype of *ndc1-39* cells, whereas the mutations T14M, M457T, and F643L were not necessary to generate the *ts* phenotype. The *ndc1-39* allele was integrated into the chromosome at the *NDC1* locus more than once in a tandem array (see Discussion). While the growth of *ndc1-39* cells was comparable to that of wild-type *NDC1* cells at the permissive temperature of 23°C (Fig. 2B, left panel), unlike wild-type cells, *ndc1-39* cells were unable to grow at the restrictive temperature of 35°C (Fig. 2B, right panel).

The subcellular localization and protein level of Ndc1-39p were compared with those of wild-type Ndc1p to ensure that the temperature sensitivity of *ndc1-39* cells was not due simply to mislocalization or diminished levels of Ndc1-39p. Log-phase cells containing either Ndc1p or Ndc1-39p tagged with three copies of the Myc epitope and SPB component Spc42p fused with GFP were grown at 35°C for 3 h. The localization of wild-type Ndc1p at both SPBs and NPCs by IF microscopy was previous described (11) and is shown in Fig. 2C, top two rows. The subcellular localization of Ndc1-39p at 35°C (Fig. 2C, bottom two rows) was similar to that of Ndc1p. The expression levels of Ndc1p and Ndc1-39p were also equivalent by Western blot analysis at 35°C (data not shown). Therefore, *ndc1-39* is a novel allele of *NDC1* that is *ts* at 35°C, with protein localization and an expression level similar to those of the wild-type protein at the restrictive temperature.

***ndc1-39* cells fail in SPB duplication and DNA segregation at the restrictive temperature.** To understand the basis of the temperature sensitivity of *ndc1-39* cells, we first examined cell cycle progression in these cells by flow cytometry. Disruption of normal cell cycle progression is often seen for SPB duplication mutants at their restrictive temperatures (12). *NDC1* and *ndc1-39* cells were synchronized in G_1 phase with the mating pheromone alpha factor (α-factor) at 23°C. Samples were then taken every hour for 4 h after release from G_1 arrest at 23 or 35°C (Fig. 3A). Log-phase cells had normal 1n and 2n DNA peaks (Fig. 3A, cycling), while α-factor-treated cells were mostly arrested in G_1 with a 1n DNA peak (Fig. 3A, α-factor). Upon release from α-factor treatment at 23 or 35°C, *NDC1* cells (Fig. 3A, left panel) replicated their DNA, displaying a 2n DNA peak; executed mitosis and cytokinesis, returning to a 1n DNA peak; and eventually became asynchronous, with both 1n and 2n DNA peaks. The flow cytometry profile for *ndc1-39* cells at 23°C was similar to the profile for wild-type cells (data not shown). In contrast, *ndc1-39* cells (Fig. 3A, right panel) transiently arrested in mitosis at 37°C, with a 2n DNA peak, 2 to 3 h after α-factor release. Then, instead of the reappearance

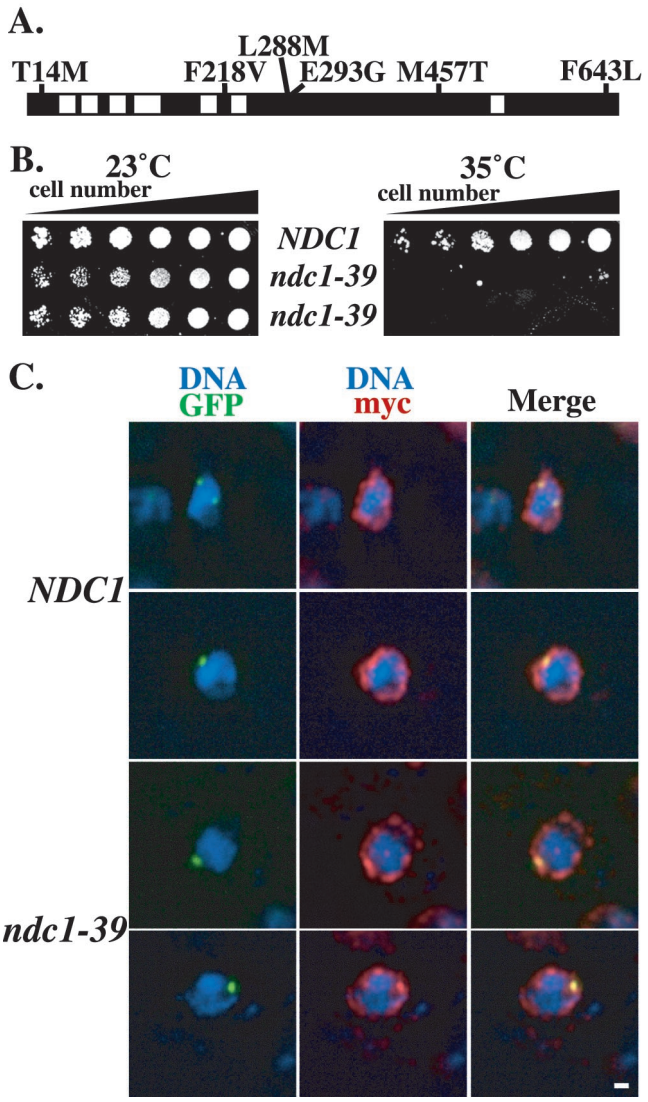

FIG. 2. *ndc1-39* is a novel temperature-sensitive (*ts*) allele of *NDC1*. (A) Six amino acid changes in the *ndc1-39* allele are shown. The black and white bars represent the structure of *NDC1* as described for Fig. 1. (B) Suspensions of *NDC1* (strain 1264) and *ndc1-39* (strain 2710) cells were plated on YPD plates at an optical density at 600 nm of 3.0 in fivefold serial dilutions and were grown at the permissive temperature of 23°C (left) and at the restrictive temperature of 35°C (right) for 3 days. Two isolates of *ndc1-39* mutants are shown. (C) Subcellular localization of Ndc1p and Ndc1-39p as visualized by IF microscopy. *NDC1* (strain 3451; top two rows) and *ndc1-39* (strain 3452; bottom two rows) cells were shifted to 35°C for 3 h in YPD medium. Ndc1p and Ndc1-39p cells tagged with the Myc epitope are shown in red (see Materials and Methods), DNA is shown in blue, autofluorescence of Spc42p tagged with GFP is shown in green, and colocalization of Spc42p-GFP with either Ndc1p-myc or Ndc1-39p-myc is shown in yellow. Each image shown was projected from five consecutive images taken at 0.1-μm intervals along the *z* axis that have been deconvolved. The *ndc1-39* allele used for this experiment did not include the F643L amino acid change that does not contribute to the *ts* phenotype. Bar, 1 μm.

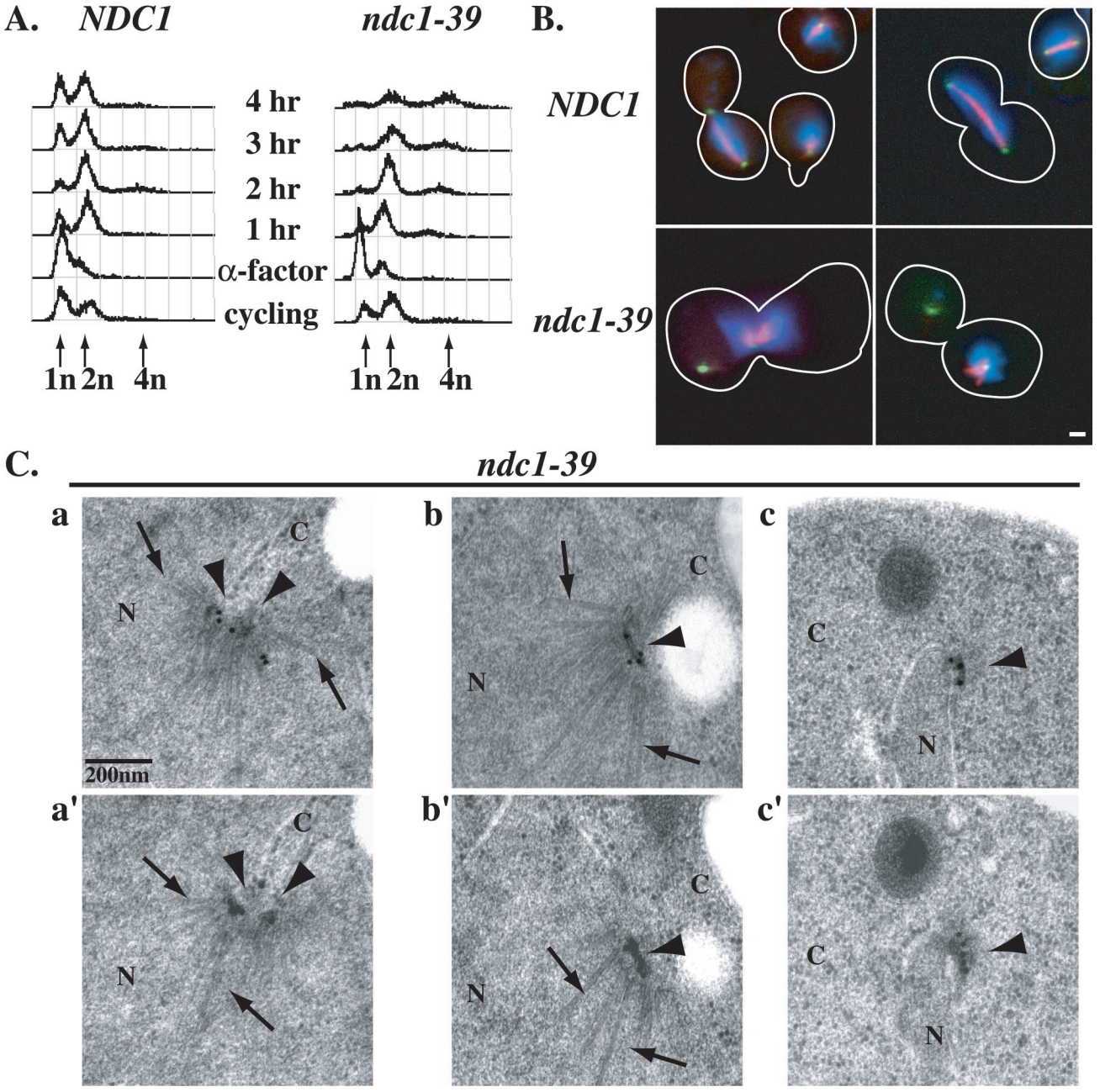

FIG. 3. *ndc1-39* cells fail in SPB duplication and DNA segregation at the restrictive temperature. (A) Cell cycle progression of *NDC1* (strain 2804; left) and *ndc1-39* (strain 3447; right) cells as monitored by flow cytometry. Log-phase (cycling) *NDC1* and *ndc1-39* cells grown in YPD medium were synchronized in G_1 with α-factor at 23°C for 3 h and then released into the restrictive temperature of 35°C, and samples were taken every hour for 4 h. The *x* axis represents DNA content, and the *y* axis for each time point represents the number of cells in a population with a given DNA content. Pre (1n)-, post (2n)-, and endo (4n)-replication DNA peaks are indicated by arrows. Consistent with the mitotic arrest in *ndc1-39* cells at 35°C at 3 h after α-factor release, 69% ($n = 200$) of *ndc1-39* cells accumulated with a large-budded morphology, compared to 37% ($n = 200$) of *NDC1* cells. *NDC1* and *ndc1-39* cells from the 2-h time point in panel A were examined by IF microscopy (B), and by IEM (C). Spc42p fused with GFP was used to identify SPBs. (B) Microtubules in *NDC1* (top row) and *ndc1-39* (bottom row) cells were labeled in red, DNA was labeled in blue, and SPBs were labeled in green (see Materials and Methods). The morphology of the cells is outlined in white. Bar, 1 μm. (C) Immunoelectron micrographs a and a′, b and b′, and c and c′ are images of two consecutive serial sections of *ndc1-39* cells (strain 3448). b, b′, c, and c′ are images showing the two SPBs of one cell. SPBs (arrowheads) are immunolabeled and identified by a GFP antibody to Spc42p-GFP and a colloidal gold-conjugated secondary antibody. Examples of nuclear microtubules are indicated by arrows. N, nucleoplasm; C, cytoplasm. Bar, 0.2 μm.

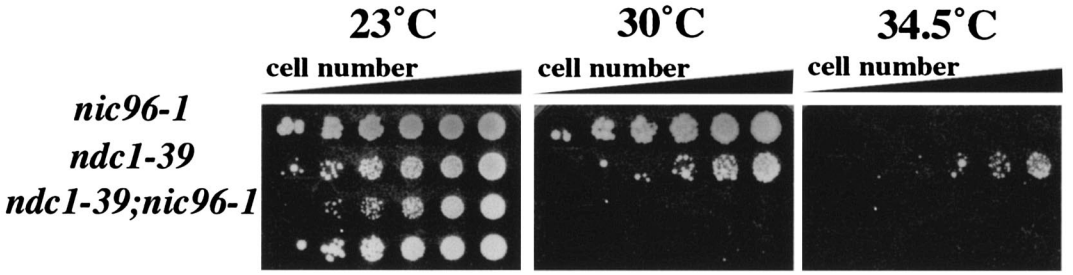

FIG. 4. *ndc1-39* exhibits genetic interaction with *nic96-1*. Suspensions of *nic96-1* (strain 2252), *ndc1-39* (strain 2710), and *ndc1-39 nic96-1* (strains 3538 and 3539) cells were plated at an optical density at 600 nm of 3.0 in fivefold serial dilutions on plates containing synthetic medium lacking leucine and were grown at the permissive temperature of 23°C (left), at 30°C (middle), or at 34.5°C (right) for 3 days. Two strains of *ndc1-39 nic96-1* mutants are shown.

of a 1n DNA peak, a 4n DNA peak was observed 4 h after α-factor release. This increase-in-ploidy, or endoreplication, phenotype has been observed for a number of SPB duplication mutants, including *ndc1-1* and *mps2-1* (12). It is also seen when *NDC1* functioning is compromised by either increasing (10) or decreasing (35) the *NDC1* gene dosage.

We determined if the disruption of normal cell cycle progression and the increase-in-ploidy phenotype could be due to a failure in DNA segregation by examining the spindle structure in *ndc1-39* cells at 35°C by IF microscopy. In *NDC1* cells, both normal short and long mitotic spindles were readily observed 2 h after the release from α-factor treatment at 35°C (Fig. 3B, top row), and DNAs in these cells were segregated into two equal masses. However, no mitotic spindles were observed in *ndc1-39* cells at the same time point (Fig. 3B, bottom row), even though the DNA contents of *NDC1* and *ndc1-39* cells were similar (Fig. 3A). Spc42p fused with GFP was used to identify SPBs (Fig. 3B). In 92% ($n = 200$) of the large-budded *ndc1-39* cells that had two distinct Spc42p-GFP signals, all of the DNA was associated with only the one of the two SPBs that was often located near the bud neck. Astral microtubules were associated with one (along with the DNA mass) or both of the SPBs. This monopolar spindle phenotype is similar to that observed in *ndc1-1*, *mps2-1*, and *bbp1-1* cells at their restrictive temperatures (32, 39, 40). The original SPB is still able to nucleate nuclear microtubules that associate with chromosomes and acts as a spindle pole, but the newly synthesized SPB is defective in forming nuclear microtubules and does not function as a spindle pole. The monopolar spindle phenotype was occasionally seen (<5%; $n = 200$) in *ndc1-39* cells at 23°C and was not observed in wild-type cells.

We performed IEM with *ndc1-39* cells 2 h after α-factor release at 35°C to examine the structure of SPBs more closely (Fig. 3C). To be certain of identifying any incomplete or aberrant SPB structures, we immunolabeled Spc42p-GFP as an SPB marker. Wild-type cells with large buds should have completed SPB duplication and separation (1, 12). However, two abnormal phenotypes were seen for *ndc1-39* cells. Of the 15 large-budded cells examined, 7 had two adjacent SPB structures (Fig. 3C, panels a and a′) that appeared to have split from a single SPB, since no half-bridge, which normally connects side-by-side SPBs that have not separated, could be detected. In addition, the nuclear envelope invaginated at these SPBs and nuclear microtubules splayed out (Fig. 3C, panel a, arrows). In the other eight cells examined, two separate SPBs were observed (Fig. 3C, panels b, b′, c, and c′). One of the SPBs contained normal layered structures embedded in the nuclear envelope and was often seen near the bud neck (Fig. 3C, panels b and b′). This was consistent with the existing functional SPB that forms the monopolar spindle, since it was capable of nucleating both cytoplasmic and nuclear microtubules (Fig. 3C, panels b and b′, arrows). The other SPB contained a partial SPB structure typically located at the tip of the thin nuclear envelope extension (Fig. 3C, panels c and c′). The structure resided on the cytoplasmic side of the nuclear envelope and was not able to nucleate nuclear microtubules. This defective SPB resembled a duplication plaque, and it was separated from the functional SPB by cytoplasmic microtubules that it could still form (40). The cytoplasmic microtubules are also likely to contribute to the abnormal shape of the nuclear envelope in these monopolar mutants by pulling the defective SPB with attached nuclear envelope away from the functional SPB (40). This SPB duplication defect observed in *ndc1-39* cells is very similar to previously reported defects in *ndc1-1*, *bbp1-1*, and *mps2-1* cells (32, 39, 40). The IEM data reported here are consistent with the results from the IF studies (Fig. 3B), and taken together, these results show that *ndc1-39* cells are defective in insertion of the SPB during SPB duplication at 35°C.

***ndc1-39* exhibits genetic interaction with *nic96-1*.** We sought to determine if *ndc1-39* cells also exhibited phenotypes associated with the disruption of NPC functions in addition to SPB duplication defects. We first examined the genetic interactions between *ndc1-39* and mutant alleles in candidate nucleoporins. The deletion of *POM152* or *POM34*, genes that encode the other two pore membrane proteins besides *NDC1* (28), showed neither suppression nor a synthetic lethal phenotype with *ndc1-39* (data not shown). Similarly, *ndc1-39* was not synthetically lethal with the *nup192-15* mutation that causes NPC assembly defects (22; data not shown). However, *ndc1-39* exhibited enhanced growth defects with another NPC assembly mutation, *nic96-1* (44), at a semipermissive temperature (Fig. 4). While *nic96-1* or *ndc1-39* single mutants were able to grow at 30°C, double mutants were unable to grow (Fig. 4). This result demonstrates that *NDC1* and *NIC96* genetically interact and suggests that Ndc1p may be involved in NPC assembly or some other NPC-associated function.

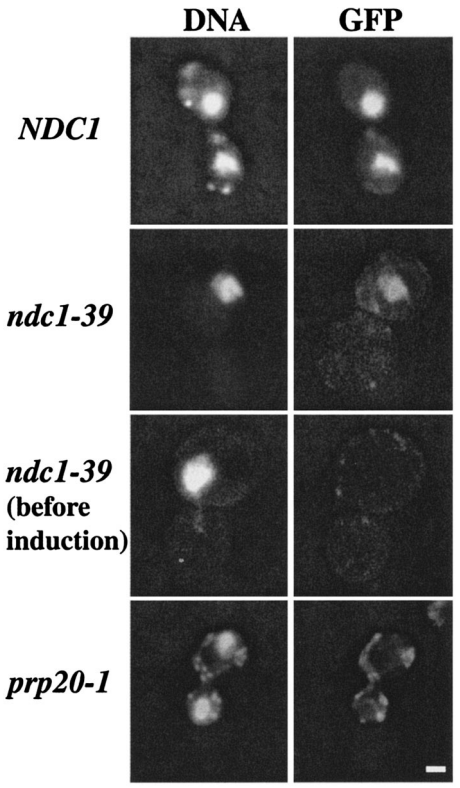

FIG. 5. *ndc1-39* cells have normal nuclear protein import at the restrictive temperature. *NDC1* (strain 2568/pJON280; first row), *ndc1-39* (strain 3446/pJON280; second and third rows), and *prp20-1* (strain 2925/pJON280; fourth row) (21) cells were grown at 35°C for 5 h in raffinose-containing medium that lacked uracil. Galactose was then added to induce the expression of the H2B1-GFP reporter (31) for 2 h, and cells were processed for fluorescence microscopy. DNA staining is shown in the left column, and GFP staining is shown in the right column. Bar, 1 μm.

***ndc1-39* cells have normal nuclear protein import at the restrictive temperature.** A nuclear protein import assay was performed to check the NPC transport function in *ndc1-39* cells. A galactose-inducible GFP construct that contained the nuclear localization signal from histone H2B1 (pJON280) was used as a reporter to determine if the GFP protein was properly translated and transported into the nucleus upon induction with galactose (31). Cells with a mutation in the *PRP20* gene were used as a positive control for the phenotype since they have been shown to have nuclear protein import and mRNA export defects (21). Asynchronously growing *NDC1*, *ndc1-39*, and *prp20-1* cells were shifted to 35°C for 5 h, at which time galactose was added for 2 h to induce the expression of the GFP reporter. The cells were then processed for fluorescence microscopy to determine the subcellular localization of the GFP reporter. The GFP signal coincided with DNA staining in both *NDC1* (Fig. 5, first row) and *ndc1-39* cells (Fig. 5, second row), indicating that the GFP reporter had been imported into the nucleus and that the transport function was normal in these cells. No GFP signal was observed in *NDC1* or *ndc1-39* cells before galactose induction (Fig. 5, third row; also data not shown). Note that *ndc1-39* cells were shifted to 35°C for 5 h before galactose induction of the GFP reporter to ensure that Ndc1-39p was inactivated, as evidenced by the appearance of large-budded cells with only one mass of DNA (Fig. 5, second and third rows). No nuclear GFP signal was observed in the control *prp20-1* cells (Fig. 5, fourth row) (21). In conclusion, *ndc1-39* cells exhibit normal import of the induced GFP reporter protein into the nucleus and hence normal mRNA export from the nucleus at the restrictive temperature.

***ndc1-39* cells have normal NPC distribution at the restrictive temperature.** Next, the distribution of NPCs was monitored by using a constitutively expressed GFP-tagged nucleoporin, Nup49p, as a marker for NPCs in *NDC1*, *ndc1-39*, and *nup133*Δ cells. *nup133*Δ cells were used as a positive control for the phenotype since these cells have been shown to have NPC distribution defects (2, 7). The cells were grown at 23 or 35°C for 3 to 4 h and then processed for fluorescence microscopy. A punctate perinuclear Nup49p-GFP signal was observed in both *NDC1* and *ndc1-39* cells at 35°C (Fig. 6, first and second rows). This indicates that NPCs were distributed normally in these cells. In contrast, Nup49p-GFP clustered as one or two spots in *nup133*Δ cells even at 23°C (Fig. 6, third row), as was expected because of their NPC distribution defects (2, 7). We conclude that there are no NPC distribution defects in *ndc1-39* cells at the restrictive temperature (also see Fig. 8).

***ndc1-39* cells fail to assemble Nup49p-GFP into NPCs at the restrictive temperature.** To determine if NPC assembly is affected in *ndc1-39* mutants, we examined the incorporation of a newly synthesized nucleoporin into NPCs in an NPC assembly assay derived from a previously described method (11). *NDC1* and *ndc1-39* cells containing galactose-inducible GFP-tagged *NUP49* were grown at 23 or 35°C, and galactose was added to the medium to induce the expression of Nup49p-GFP. The cells were then shifted to medium containing glucose to further repress the expression of Nup49p-GFP. The newly synthesized Nup49p-GFP was allowed to assemble into NPCs, and the distribution of Nup49p-GFP was visualized by fluorescence microscopy at various stages of the experiment (Fig. 7A). In *NDC1* cells after galactose induction at 35°C, a punctate perinuclear Nup49p-GFP signal was readily observed (Fig. 7A, panel a), along with a faint signal throughout the cytoplasm. After the repression of Nup49p-GFP expression in the presence of glucose, 96% of the cells had incorporated Nup49p-GFP into NPCs, producing a punctate perinuclear signal (Fig. 7A, panel b). Interestingly, the majority of *ndc1-39* cells had intense spots of Nup49p-GFP signals after galactose induction at 35°C (Fig. 7A, panels c and e, arrows), but some cells had a normal punctate perinuclear signal (Fig. 7A, panels c and e). The aggregate phenotype was more apparent after the cells were grown in glucose-containing medium. Sixty percent of the *ndc1-39* cells had one or more intense Nup49p-GFP signals (Fig. 7A, panels d and f, arrows), leaving only 40% of the *ndc1-39* cells with an apparent normal punctate perinuclear distribution of Nup49p-GFP (Fig. 7A, panels d and f). The Nup49p-GFP aggregates may represent Nup49p-GFP that is not properly assembled into NPCs. Quantification of the data is shown in Fig. 7B. In addition, 24% of *ndc1-39* cells failed to assemble Nup49p-GFP into NPCs at 23°C (Fig. 7B). Western blot analysis indicated that Nup49p-GFP was expressed at the same level in both *NDC1* and *ndc1-39* cells at 35°C (data not shown).

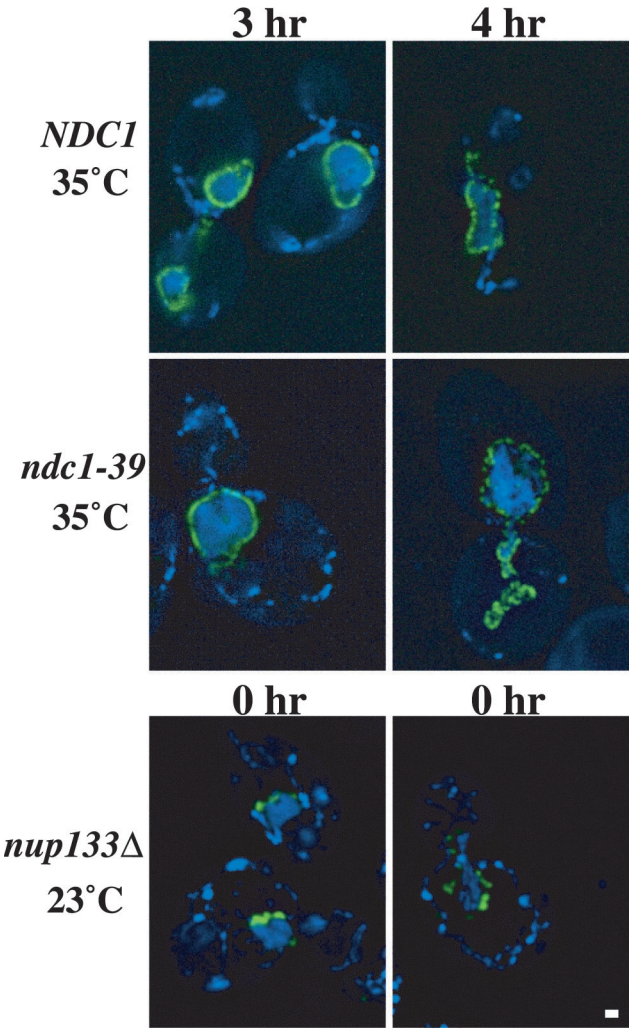

FIG. 6. *ndc1-39* cells have normal NPC distribution at the restrictive temperature. *NDC1* (strain 3345; first row) and *ndc1-39* (strain 3346; second row) cells grown in YPD medium were shifted to 35°C for 3 h (left column) or 4 h (right column), whereas *nup133*Δ (strain 1258; third row) cells were grown at 23°C throughout the experiment. The cells were then processed for fluorescence microscopy. Two images of *nup133*Δ cells at the beginning of the experiment (0 h) are shown. DNA is shown in blue and Nup49p-GFP is shown in green. Each image shown was projected from five consecutive planes taken at 0.1-μm intervals along the *z* axis that have been deconvolved. Bar, 1 μm.

We also examined the incorporation of Nup49p-GFP in *ndc1-1* cells, in which NPC assembly has been shown to be normal, at the restrictive temperature of 15°C (11). The NPC assembly assay was performed at the permissive temperature of 30°C, similarly to the control experiment conducted at 23°C as described above. Only 11% of the *ndc1-1* cells at 30°C and 20% of the *ndc1-1* cells at 15°C failed to incorporate Nup49p-GFP properly into NPCs (Fig. 7B), compared to 60% of *ndc1-39* cells at 35°C (Fig. 7B). These results indicate that the abnormal assembly of Nup49p-GFP into NPCs is specific to cells containing the *ndc1-39* allele but not the *ndc1-1* allele.

To better understand the nature of Nup49p-GFP aggregates in *ndc1-39* cells, we processed *NDC1* and *ndc1-39* cells for IEM after growing them in glucose-containing medium at 35°C. Nup49p-GFP was immunolabeled with an anti-GFP primary antibody and a colloidal gold-conjugated secondary antibody (see Materials and Methods). In *NDC1* cells, Nup49p-GFP gold particles were observed at the NPCs, as expected (Fig. 8A, arrows). The normal incorporation of Nup49p-GFP into the NPCs was also detected in some *ndc1-39* cells (Fig. 8B and C, arrows). The NPCs appeared to be distributed normally in the nuclear envelope in the *ndc1-39* cell shown (Fig. 8B), in which each of the five NPCs was labeled with at least one gold particle. Interestingly, cytoplasmic (Fig. 8C, arrowheads) and membrane-bound (Fig. 8D, arrowheads) aggregates that were labeled with gold particles were also observed. These aggregates are consistent with the intense GFP labeling seen by fluorescence microscopy (Fig. 7B). Occasionally, we observed Nup49p-GFP at a nuclear pore and as an aggregate in the same cell (Fig. 8C). In summary, *ndc1-39* cells exhibit defects in assembling Nup49p-GFP into NPCs at 35°C, by which a fraction of the Nup49p-GFP is misassembled and forms aggregates in the cell.

DISCUSSION

In this study, we investigated the role of Ndc1p, the only integral membrane protein that localizes to both the SPBs and NPCs, in both SPB duplication and NPC-associated functions by using a novel *ts* allele of *NDC1*, *ndc1-39*. We found that *ndc1-39* cells are defective in SPB duplication and likely in NPC assembly at the restrictive temperature of 35°C, consistent with the idea that Ndc1p is required for the insertion of both the SPBs and NPCs into the nuclear envelope.

***NDC1* functional domains.** We created seven serial *NDC1* truncation proteins and found that only one small region, between amino acids 368 and 466, is dispensable for both *NDC1* localization and function. This region does not contain any of the seven predicted transmembrane domains. The other six deletions of *NDC1* rendered Ndc1p nonfunctional and did not localize properly. One possible explanation is that most of the truncation proteins lack one or two of the seven predicted transmembrane domains that are likely required for proper localization. Similarly, the mutations might have affected the topology of the protein in the nuclear envelope.

***NDC1* in SPB duplication.** Ndc1-39p is expressed and localized similarly to the wild-type protein at the restrictive temperature. However, *ndc1-39* cells are defective in SPB duplication in that the newly synthesized SPB is similar to the duplication plaque but fails to be inserted into the nuclear envelope. Consequently, these cells exhibit transient mitotic arrest due to failure in bipolar spindle formation, DNA segregation defects, and an increase-in-ploidy phenotype.

Interestingly, the *ndc1-39* allele was found to be integrated two or more times in a tandem array as verified by Southern blot analysis. Cells containing a single copy of the *ndc1-39* allele were not identified because the Ndc1p function in these cells might have been compromised at the permissive temperature such that single-copy integrants were sick or inviable. However, these defects would be overcome by slightly increasing the *NDC1* gene dosage. Wild-type or mutant alleles of *NDC1* are known to be very sensitive to gene dosage (10).

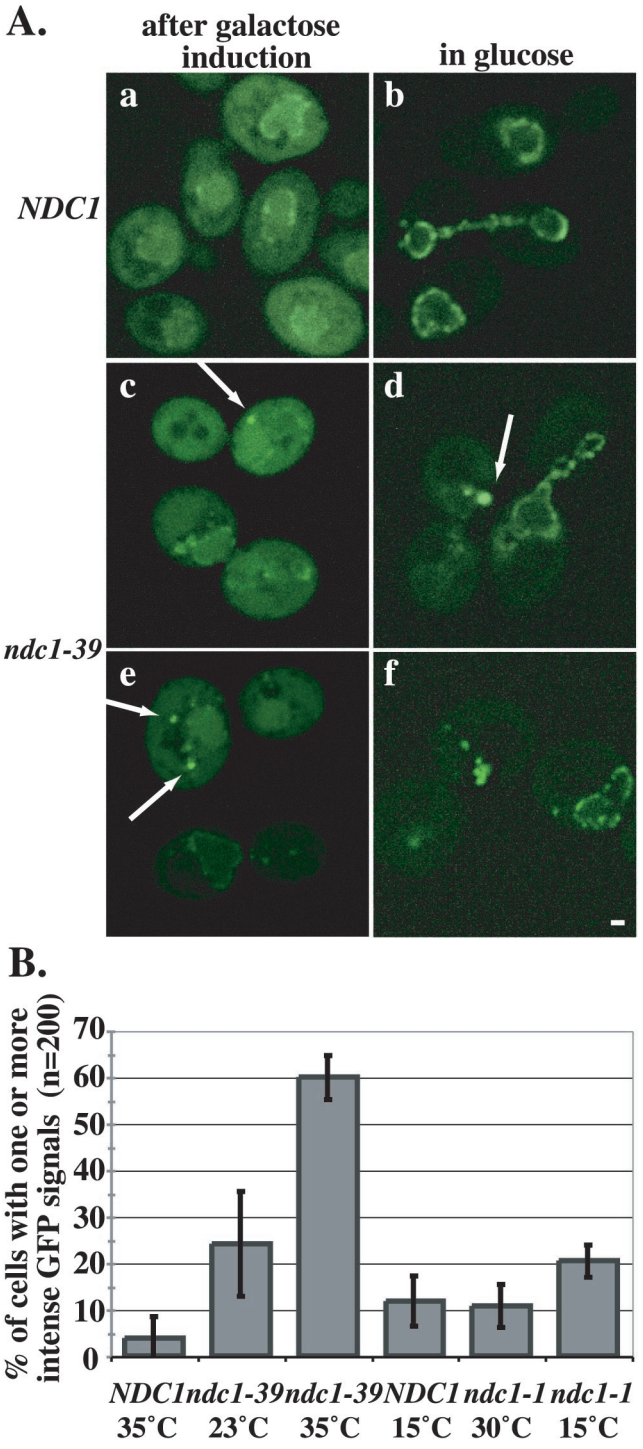

FIG. 7. *ndc1-39* cells fail to assemble Nup49p-GFP into NPCs at the restrictive temperature. (A) Log-phase *NDC1* (strain 3245; a and b) and *ndc1-39* (strain 3244; c to f) cells were grown in raffinose-containing medium at 23 or 35°C for 2.5 h, and galactose was added to induce the expression of Nup49p-GFP for 1.5 h (a, c, and e). The cells were then grown in YPD medium for 2 h to repress further Nup49p-GFP expression (b, d, and f). The distribution of Nup49p-GFP (green) was visualized by fluorescence microscopy. Nup49p-GFP clusters as one or two aggregates in *ndc1-39* cells (c to f, arrows). Each image shown was projected from eight consecutive images taken at 0.1-μm intervals along the *z* axis that have been deconvolved. Bar, 1 μm. (B) Quantification of the data in panel A. The *y* axis represents the percentages of cells ($n = 200$) with one or more intense Nup49p-GFP signals for *NDC1* cells at 35°C, *ndc1-39* cells at 23°C, and *ndc1-39* cells at 35°C. *ndc1-39* cells at 23°C were grown in YPD medium for 4 h. *NDC1* and *ndc1-1* cells (strain 3299) were grown in raffinose-containing medium for 16.5 h at 15°C, and galactose was added for 11 h to induce the expression of Nup49p-GFP. Then the cells were grown in YPD medium for 6 h. A control at the permissive temperature of 30°C was performed similarly to the 23°C control, as described above. The percentages of *NDC1* cells at 15°C, *ndc1-1* cells at 30°C, and *ndc1-1* cells at 15°C that had Nup49p-GFP assembly defects are also shown. Error bars are based on three independent trials for the experiments conducted at 23 and 35°C and two independent trials for the experiments conducted at 30 and 15°C.

Regardless of the copy number of the *ndc1-39* allele, Ndc1-39p was expressed at a level similar to that of Ndc1p. In addition, *ndc1-39* cells were healthy at the permissive temperature but still *ts*, thus allowing analysis of their mutant phenotypes at the restrictive temperature.

The study of *ndc1-39* further validates the requirement for Ndc1p in the insertion step of the duplication plaque into the nuclear envelope during SPB duplication (see below for a proposed mechanism).

***NDC1* in NPC assembly.** The existing alleles for *NDC1*, *ndc1-1* (11) and *ndc1-39*, do not reveal a role for *NDC1* in nuclear transport or in the distribution of NPCs in the nuclear envelope. However, Ndc1p seems to be involved in NPC assembly, since *ndc1-39* mutants showed an enhanced growth defect in combination with *nic96-1* mutants and had Nup49p-GFP assembly defects.

Even though the precise mechanism of NPC assembly is not known, studies from vertebrate systems suggest that the two pore membrane proteins, POM121 and gp210, play an important role during NPC assembly (3, 8, 13, 34, 36). The membrane proteins could trigger pore formation by facilitating the fusion of the inner and outer membranes of the nuclear envelope and allowing the assembly of other nucleoporins. Although there are no POM121 and gp210 homologues in yeast, the pore membrane proteins Ndc1p, Pom152p, and Pom34p could perform analogous functions (28). However, unlike *NDC1*, cells grow normally when *POM152* or *POM34* is deleted (42).

We propose that the essential integral membrane protein Ndc1p functions similarly during both SPB duplication and NPC assembly. Ndc1p could mediate the fusion between the inner and outer nuclear membranes by interacting with itself or other proteins to stabilize the fenestra in the nuclear envelope, thus allowing the assembly of nucleoporins at the NPCs or the insertion of the duplication plaque and the recruitment of nuclear SPB components to the SPBs. However, attempts to identify SPB or NPC components that interact with Ndc1p biochemically have not been successful thus far. It is also not known whether the assembly of other nucleoporins or nuclear pore subcomplexes, in addition to that of *NUP49*, is affected in *ndc1-39* cells.

In NPC assembly mutants such as *nic96-1* and *nup192-15* (7, 15, 22, 44), a decrease in NPC numbers and a marked decrease in the autofluorescence level of endogenously expressed Nup49p-GFP are observed as these cells continue to divide for several generations at the restrictive temperature, and the pre-

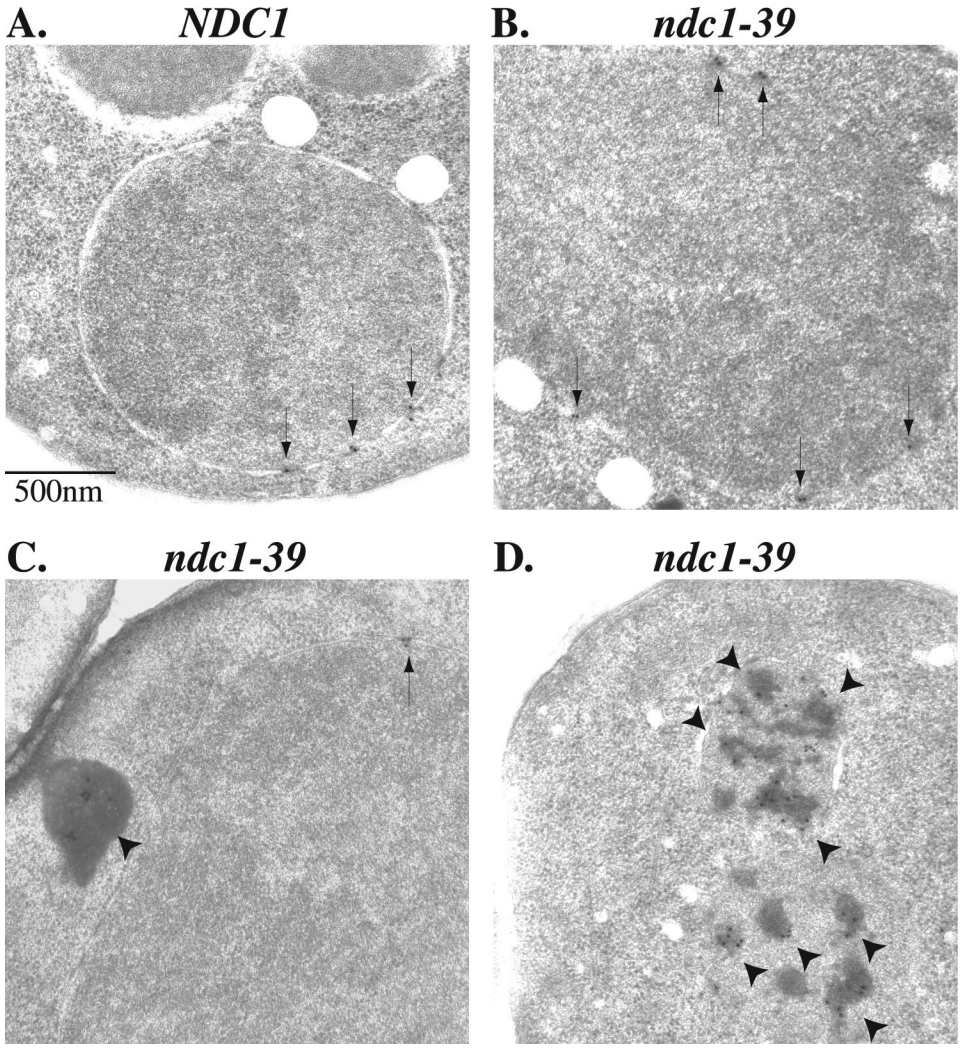

FIG. 8. IEM of Nup49p-GFP assembly in *NDC1* and *ndc1-39* cells at the restrictive temperature. Experiments were performed as described for Fig. 7. Nup49p-GFP was immunolabeled with an antibody to GFP and visualized with a colloidal gold-conjugated secondary antibody in *NDC1* (A) and *ndc1-39* (B to D) cells after the repression of Nup49p-GFP expression in YPD medium. At 35°C, Nup49p-GFP was localized correctly to the nuclear pores (arrows) in *NDC1* cells (A) and in some of the *ndc1-39* cells (B and C). Nup49p-GFP labeling was also observed seven times as aggregates in the cytoplasm (arrowheads in panel C) and four times as membrane-bound aggregates (arrowheads in panel D) in the 15 *ndc1-39* cells examined. Bar, 0.5 μm.

existing NPCs are titrated into daughter cells after each cell division. The number of NPCs did not seem to decrease in *ndc1-39* cells during the first cell cycle upon shifting to the restrictive temperature, since we observed a wild-type level of Nup49p-GFP signal in *ndc1-39* cells. The number of NPCs and the signal of endogenously expressed Nup49p-GFP might have decreased if *ndc1-39* cells were able to continue cycling at the restrictive temperature. However, it is not possible to determine if the number of NPCs decreased in *ndc1-39* cells in subsequent cell cycles at the restrictive temperature because these cells failed in SPB duplication and went through lethal mitosis during the first cell cycle. Nonetheless, by a different method of monitoring NPC assembly using galactose-inducible Nup49p-GFP, we were able to demonstrate the potential involvement of Ndc1p in NPC assembly that could not be detected otherwise.

Sixty percent of the *ndc1-39* cells had defects in incorporating Nup49p-GFP into NPCs at the restrictive temperature, as indicated by the presence of Nup49p-GFP aggregates instead of the normal punctate perinuclear signal. We do not believe that the Nup49p-GFP assembly defect seen in *ndc1-39* cells at the restrictive temperature is a secondary effect due to a failure in SPB duplication and arrest in mitosis, since *ndc1-1* cells exhibited SPB duplication defects but no effects on NPC assembly, consistent with a previous analysis of *ndc1-1* (11). By IEM, aggregates of Nup49p-GFP observed in *ndc1-39* cells at the restrictive temperature often did not reside at the nuclear pores, but rather were located in the cytoplasm or a membrane-bound structure (Fig. 8D). Neither the cytoplasmic aggregates nor the membrane-limited structures were observed when Nup49p-GFP was induced in wild-type cells. The membranes may represent an expansion of the nuclear envelope or

the endoplasmic reticulum. However, in our preparation, we did not detect the double membrane lamella structure observed when Nup53p is overexpressed (24). It is possible that these aggregates of Nup49p-GFP represent NPC assembly intermediates.

Interestingly, 40% of the *ndc1-39* cells seemed to incorporate newly synthesized Nup49p-GFP into the NPCs normally (Fig. 8B). There are several possibilities to explain why Nup49p-GFP assembly was not defective in all *ndc1-39* cells. First, the punctate perinuclear Nup49p-GFP signal observed could reflect the exchange of newly synthesized Nup49p-GFP into the preexisting functional NPCs instead of de novo NPC synthesis (2, 6). Another possibility is that in some of the cells, Ndc1-39p was not fully inactivated at the time when synthesis of Nup49p-GFP was induced, or there may have been a lag from the time that Ndc1-39p became nonfunctional to the time when the mutant phenotype was observed. A third possibility is that Nup49p-GFP was incorporated into partially formed or nonfunctional NPCs that still appeared to be embedded in the nuclear envelope and that cannot be distinguished from normal NPCs in our assay.

In conclusion, we have demonstrated that *NDC1*, encoding the only essential integral nuclear envelope membrane protein common to both SPBs and NPCs, is required for SPB duplication and possibly for NPC assembly. We also provided evidence to support the idea that Ndc1p is important for the insertion of both organelles into the nuclear envelope and that it serves as an important link for understanding the biogenesis of SPBs and NPCs.

ACKNOWLEDGMENTS

We thank Don Cleveland, Jason Kahana, Pamela Silver, and Susan Wente for various reagents. We also thank Harold Fisk and Michele Jones for critical reading of the manuscript.

This work was supported by National Institutes of Health grant GM-59992 (to M.W.) and National Institutes of Health training grant GM-07135 (to C.K.L.).

REFERENCES

1. **Adams, I. R., and J. V. Kilmartin.** 2000. Spindle pole body duplication: a model for centrosome duplication? Trends Cell Biol. **10:**329–335.
2. **Belgareh, N., and V. Doye.** 1997. Dynamics of nuclear pore distribution in nucleoporin mutant yeast cells. J. Cell Biol. **136:**747–759.
3. **Bodoor, K., S. Shaikh, D. Salina, W. H. Raharjo, R. Bastos, M. Lohka, and B. Burke.** 1999. Sequential recruitment of NPC proteins to the nuclear periphery at the end of mitosis. J. Cell Sci. **112:**2253–2264.
4. **Boeke, J. D., J. Trueheart, G. Natsoulis, and G. R. Fink.** 1987. 5-Fluoroorotic acid as a selective agent in yeast molecular genetics. Methods Enzymol. **154:**164–175.
5. **Brachmann, C. B., A. Davies, G. J. Cost, E. Caputo, J. Li, P. Hieter, and J. D. Boeke.** 1998. Designer deletion strains derived from *Saccharomyces cerevisiae* S288C: a useful set of strains and plasmids for PCR-mediated gene disruption and other applications. Yeast **14:**115–132.
6. **Bucci, M., and S. R. Wente.** 1997. In vivo dynamics of nuclear pore complexes in yeast. J. Cell Biol. **136:**1185–1199.
7. **Bucci, M., and S. R. Wente.** 1998. A novel fluorescence-based genetic strategy identifies mutants of *Saccharomyces cerevisiae* defective for nuclear pore complex assembly. Mol. Biol. Cell **9:**2439–2461.
8. **Burke, B., and J. Ellenberg.** 2002. Remodelling the walls of the nucleus. Nat. Rev. Mol. Cell. Biol. **3:**487–497.
9. **Castillo, A. R., J. B. Meehl, G. Morgan, A. Schutz-Geschwender, and M. Winey.** 2002. The yeast protein kinase Mps1p is required for assembly of the integral spindle pole body component Spc42p. J. Cell Biol. **156:**453–465.
10. **Chial, H. J., T. H. Giddings, Jr., E. A. Siewert, M. A. Hoyt, and M. Winey.** 1999. Altered dosage of the *Saccharomyces cerevisiae* spindle pole body duplication gene, *NDC1*, leads to aneuploidy and polyploidy. Proc. Natl. Acad. Sci. USA **96:**10200–10205.
11. **Chial, H. J., M. P. Rout, T. H. Giddings, Jr., and M. Winey.** 1998. *Saccharomyces cerevisiae* Ndc1p is a shared component of nuclear pore complexes and spindle pole bodies. J. Cell Biol. **143:**1789–1800.
12. **Chial, H. J., and M. Winey.** 1999. Mechanisms of genetic instability revealed by analysis of yeast spindle pole body duplication. Biol. Cell **91:**439–450.
13. **Drummond, S. P., and K. L. Wilson.** 2002. Interference with the cytoplasmic tail of gp210 disrupts "close opposition" of nuclear membranes and blocks nuclear pore dilation. J. Cell Biol. **158:**53–62.
14. **Giddings, T. H., Jr., E. T. O'Toole, M. Morphew, D. N. Mastronarde, J. R. McIntosh, and M. Winey.** 2001. Using rapid freeze and freeze-substitution for the preparation of yeast cells for electron microscopy and three-dimensional analysis. Methods Cell Biol. **67:**27–42.
15. **Gomez-Ospina, N., G. Morgan, T. H. Giddings, Jr., B. Kosova, E. Hurt, and M. Winey.** 2000. Yeast nuclear pore complex assembly defects determined by nuclear envelope reconstruction. J. Struct. Biol. **132:**1–5.
16. **Guthrie, C., and G. R. Fink (ed.).** 2002. Methods in enzymology, vol. 350. Guide to yeast genetics and molecular and cell biology. Academic Press Inc., San Diego, Calif.
17. **Hutter, K. J., and H. E. Eipel.** 1979. Microbial determinations by flow cytometry. J. Gen. Microbiol. **113:**369–375.
18. **Jaspersen, S. L., T. H. Giddings, Jr., and M. Winey.** 2002. Mps3p is a novel component of the yeast spindle pole body that interacts with the yeast centrin homologue Cdc31p. J. Cell Biol. **159:**945–956.
19. **Kilmartin, J. V.** 2003. Sfi1p has conserved centrin-binding sites and an essential function in budding yeast spindle pole body duplication. J. Cell Biol. **162:**1211–1221.
20. **Knop, M., K. Siegers, G. Pereira, W. Zachariae, B. Winsor, K. Nasmyth, and E. Schiebel.** 1999. Epitope tagging of yeast genes using a PCR-based strategy: more tags and improved practical routines. Yeast **15:**963–972.
21. **Koepp, D. M., D. H. Wong, A. H. Corbett, and P. A. Silver.** 1996. Dynamic localization of the nuclear import receptor and its interactions with transport factors. J. Cell Biol. **133:**1163–1176.
22. **Kosova, B., N. Pante, C. Rollenhagen, and E. Hurt.** 1999. Nup192p is a conserved nucleoporin with a preferential location at the inner site of the nuclear membrane. J. Biol. Chem. **274:**22646–22651.
23. **Kunkel, T. A., J. D. Roberts, and R. A. Zakour.** 1987. Rapid and efficient site-specific mutagenesis without phenotypic selection. Methods Enzymol. **154:**367–382.
24. **Marelli, M., C. P. Lusk, H. Chan, J. D. Aitchison, and R. W. Wozniak.** 2001. A link between the synthesis of nucleoporins and the biogenesis of the nuclear envelope. J. Cell Biol. **153:**709–723.
25. **Mutvei, A., S. Dihlmann, W. Herth, and E. C. Hurt.** 1992. *NSP1* depletion in yeast affects nuclear pore formation and nuclear accumulation. Eur. J. Cell Biol. **59:**280–295.
26. **O'Toole, E. T., M. Winey, and J. R. McIntosh.** 1999. High-voltage electron tomography of spindle pole bodies and early mitotic spindles in the yeast *Saccharomyces cerevisiae.* Mol. Biol. Cell **10:**2017–2031.
27. **Rothstein, R.** 1991. Targeting, disruption, replacement, and allele rescue: integrative DNA transformation in yeast. Methods Enzymol. **194:**281–301.
28. **Rout, M. P., J. D. Aitchison, A. Suprapto, K. Hjertaas, Y. Zhao, and B. T. Chait.** 2000. The yeast nuclear pore complex: composition, architecture, and transport mechanism. J. Cell Biol. **148:**635–651.
29. **Ryan, K. J., J. M. McCaffery, and S. R. Wente.** 2003. The Ran GTPase cycle is required for yeast nuclear pore complex assembly. J. Cell Biol. **160:**1041–1053.
30. **Ryan, K. J., and S. R. Wente.** 2002. Isolation and characterization of new *Saccharomyces cerevisiae* mutants perturbed in nuclear pore complex assembly. BMC Genet. **3:**17.
31. **Schlenstedt, G., C. Saavedra, J. D. J. Loeb, C. N. Cole, and P. A. Silver.** 1995. The GTP-bound form of the yeast RAN/TC4 homologue blocks nuclear protein import and appearance of poly(A)$^+$ RNA in the cytoplasm. Proc. Natl. Acad. Sci. USA **92:**225–229.
32. **Schramm, C., S. Elliott, A. Shevchenko, A. Shevchenko, and E. Schiebel.** 2000. The Bbp1p-Mps2p complex connects the SPB to the nuclear envelope and is essential for SPB duplication. EMBO J. **19:**421–433.
33. **Sikorski, R. S., and P. Hieter.** 1989. A system of shuttle vectors and yeast host strains designed for efficient manipulation of DNA in *Saccharomyces cerevisiae.* Genetics **122:**19–27.
34. **Suntharalingam, M., and S. R. Wente.** 2003. Peering through the pore: nuclear pore complex structure, assembly, and function. Dev. Cell **4:**775–789.
35. **Thomas, J. H., and D. Botstein.** 1986. A gene required for the separation of chromosomes on the spindle apparatus in yeast. Cell **44:**65–76.
36. **Vasu, S. K., and D. J. Forbes.** 2001. Nuclear pores and nuclear assembly. Curr. Opin. Cell Biol. **13:**363–375.
37. **Wach, A., A. Brachat, R. Pohlmann, and P. Philippsen.** 1994. New heterologous modules for classical or PCR-based gene disruptions in *Saccharomyces cerevisiae.* Yeast **10:**1793–1808.
38. **West, R. R., E. V. Vaisberg, R. Ding, P. Nurse, and J. R. McIntosh.** 1998. *cut11*$^+$: a gene required for cell cycle-dependent spindle pole body anchoring in the nuclear envelope and bipolar spindle formation in *Schizosaccharomyces pombe.* Mol. Biol. Cell **9:**2839–2855.
39. **Winey, M., L. Goetsch, P. Baum, and B. Byers.** 1991. *MPS1* and *MPS2*: novel yeast genes defining distinct steps of spindle pole body duplication. J. Cell Biol. **114:**745–754.

40. **Winey, M., M. A. Hoyt, C. Chan, L. Goetsch, D. Botstein, and B. Byers.** 1993. *NDC1*: a nuclear periphery component required for yeast spindle pole body duplication. J. Cell Biol. **122:**743–751.
41. **Winey, M., D. Yarar, T. H. Giddings, Jr., and D. N. Mastronarde.** 1997. Nuclear pore complex number and distribution throughout the *Saccharomyces cerevisiae* cell cycle by three-dimensional reconstruction from electron micrographs of nuclear envelopes. Mol. Biol. Cell **8:**2119–2132.
42. **Wozniak, R. W., G. Blobel, and M. P. Rout.** 1994. *POM152* is an integral protein of the pore membrane domain of the yeast nuclear envelope. J. Cell Biol. **125:**31–42.
43. **Yang, Q., M. P. Rout, and C. W. Akey.** 1998. Three-dimensional architecture of the isolated yeast nuclear pore complex: functional and evolutionary implications. Mol. Cell **1:**223–234.
44. **Zabel, U., V. Doye, H. Tekotte, R. Wepf, P. Grandi, and E. C. Hurt.** 1996. Nic96p is required for nuclear pore formation and functionally interacts with a novel nucleoporin, Nup188p. J. Cell Biol. **133:**1141–1152.
45. **Zeng, X., J. A. Kahana, P. A. Silver, M. K. Morphew, J. R. McIntosh, T. T. Finch, J. Carbon, and W. S. Saunders.** 1999. Slk19p is a centromere protein that functions to stabilize mitotic spindles. J. Cell Biol. **146:**415–425.